Electronic Supplementary Material (ESI) for Dalton Transactions.
This journal is © The Royal Society of Chemistry 2024

Electronic supplementary information (ESI)

Selective monooxygenation of diphosphenes with molecular oxygen: structural and bonding nature of diphosphene oxides supported by bulky Rind groups

Yuria Kawase,[a] Shota Tsujimoto,[a] Tomohiro Obayashi,[a] Satoshi Kimura,[a] Kanta Ito,[a] Shotaro Ikoma,[a] Kei Ota,[a] Daisuke Hashizume[b] and Tsukasa Matsuo*[a]

[a] *Department of Applied Chemistry, Faculty of Science and Engineering, Kindai University, 3-4-1 Kowakae, Higashi-Osaka, Osaka 577-8502, Japan*

[b] *RIKEN Center for Emergent Matter Science (CEMS), 2-1 Hirosawa, Wako, Saitama 351-0198, Japan*

E-mail: t-matsuo@apch.kindai.riken.jp

(submitted to Dalton Transactions)

Contents

1. Experimental

General Procedures

All manipulations of air- and/or moisture-sensitive compounds were performed either using standard Schlenk-line techniques or in a glove box under an inert atmosphere of argon. Anhydrous hexane, toluene and tetrahydrofuran (THF) were dried by passage through columns of activated alumina and supported copper catalyst supplied by Hansen & Co., Ltd. Deuterated benzene (benzene-d_6, C_6D_6) was dried and degassed over a potassium mirror in vacuo prior to use. O_2 gas (99.5%) was dried by passing over SICAPENT®. Other chemicals and gases were used as received. The Rind-based diphosphenes, (Eind)P=P(Eind) (**1a**) and (EMind)P=P(EMind) (**1b**), were prepared by the literature procedures.[S1]

The nuclear magnetic resonance (NMR) measurements were carried out on JEOL RESONANCE JNM-ECS400 and JNM-AL400 spectrometers (399.8 MHz for ^{1}H, 100.5 MHz for ^{13}C and 161.8 MHz for ^{31}P) and BRUKER AVANCE NEO 600 OneBay (600.1 MHz for ^{1}H, 150.9 MHz for ^{13}C and 242.9 MHz for ^{31}P). Chemical shifts (δ) are given by definition as dimensionless numbers and relative to ^{1}H or ^{13}C NMR chemical shifts of the solvent (residual C_6D_5H in C_6D_6, ^{1}H(δ) = 7.15 and ^{13}C(δ) = 128.06). The absolute values of the coupling constants are given in Hertz (Hz), regardless of their signs. Multiplicities are abbreviated as singlet (s), doublet (d), triplet (t), quartet (q), multiplet (m), and broad (br). The elemental analyses (C and H) were performed at the Materials Characterization Support Team, RIKEN Center for Emergent Matter Science and the Microanalytical Laboratory at the Institute for Chemical Research (Kyoto University). Melting points (mp) were determined by a Stanford Research Systems OptiMelt instrument and a Yazawa BY-2 instrument.

NMR Tube Reaction of (Eind)P=P(Eind) (1a) with O_2

An NMR tube equipped with a Young stopcock was charged with **1a** (20.0 mg, 24.2 μmol) and C_6D_6 (0.5 mL). The upper Ar atmosphere was replaced with O_2 gas (*ca*. 1.0–2.5 ml, 45–112 μmol). The stoppered tube was heated at 60 °C. The color of the solution gradually changed from orange to light yellow. The reaction was monitored by ^{31}P NMR spectroscopy (Fig. S1). After heating for several days to a week, the ^{31}P NMR spectrum of the reaction mixture indicated an almost quantitative conversion from **1a** to (Eind)(O=)P=P(Eind) (**2a**). After volatiles were removed in vacuo, **2a** was obtained as a light yellow solid, quantitatively. Light yellow crystals suitable for X-ray diffraction analysis were obtained by recrystallization from toluene. mp (argon atmosphere in a sealed tube) 224–226 °C (dec.); ^1H NMR (C_6D_6) δ 0.86 (t, J = 7.7 Hz, 12 H, CH_2CH_3), 0.90 (t, J = 7.8 Hz, 12 H, CH_2CH_3), 0.99 (t, J = 7.3 Hz, 12 H, CH_2CH_3), 1.00 (t, J = 7.3 Hz, 12 H, CH_2CH_3), 1.52–1.76 (m, 16 H, CH_2CH_3), 1.86 (s, 4 H, CH_2), 1.88 (s, 4 H, CH_2), 2.16–2.26 (m, 4 H, CH_2CH_3), 2.28–2.43 (m, 4 H, CH_2CH_3), 2.46–2.59 (m, 8 H, CH_2CH_3), 6.92 (*d*, $^5J_{^1H-^{31}P}$ = 2.8 Hz, 1 H, Ar*H*), 7.00 (s, 1 H, Ar*H*); ^{31}P NMR (C_6D_6) δ 60.9 (*d*, $^1J_{^{31}P-^{31}P}$ = 753 Hz), 217.7 (d, $^1J_{^{31}P-^{31}P}$ = 753 Hz). Anal. Calcd for $C_{56}H_{90}OP_2$: C, 79.95; H, 10.78. Found: C, 80.14; H, 10.82.

NMR Tube Reaction of (EMind)P=P(EMind) (1b) with O_2

An NMR tube equipped with a Young stopcock was charged with **1b** (20.0 mg, 28.0 μmol) and C_6D_6 (0.5 mL). The upper Ar atmosphere was replaced with O_2 gas (*ca*. 1.0–2.5 ml, 45–112 μmol). The stoppered tube was allowed to stand at room temperature. The color of the solution slowly changed from orange to light yellow. The reaction was monitored by ^{31}P NMR spectroscopy (Fig. S2). After several days, the ^{31}P NMR spectrum of the reaction mixture indicated an almost quantitative conversion from **1b** to (EMind)(O=)P=P(EMind) (**2b**). After volatiles were removed in vacuo, **2b** was obtained as a light yellow solid, quantitatively. Light yellow crystals suitable for X-ray diffraction analysis were obtained by recrystallization from C_6D_6. mp (argon atmosphere in a sealed tube) 247–249 °C (dec.); ^1H NMR (C_6D_6) δ ^1H NMR (C_6D_6) δ 0.79 (t, J = 7.3 Hz, 12 H, CH_2CH_3), 0.84 (t, J = 7.3 Hz, 12 H, CH_2CH_3), 1.49–1.73 (m, 16 H, CH_2CH_3), 1.83 (s, 4 H, CH_2), 1.88 (s, 4 H, CH_2), 1.94 (s, 12 H, Me), 2.00 (s, 12 H, Me), 6.89 (*d*, $^5J_{^1H–^{31}P}$ = 2.7 Hz, 1 H, Ar*H*), 6.99 (s, 1 H, Ar*H*); ^{13}C NMR (C_6D_6,) δ 9.2, 9.4, 31.3, 33.2, 33.5 (×2), 45.6 (×2), 48.2, 48.5, 53.2, 53.3, 122.1, 125.1, 149.5, 149.7, 153.6 (×2), 155.6 (×2); ^{31}P NMR (C_6D_6) δ 61.5 (*d*, $^1J_{^{31}P–^{31}P}$ = 720.0 Hz), 212.9 (d, $^1J_{^{31}P–^{31}P}$ = 720.0 Hz). Anal. Calcd for $C_{56}H_{90}OP_2$: C, 79.08; H, 10.23. Found: C, 78.84; H, 10.11.

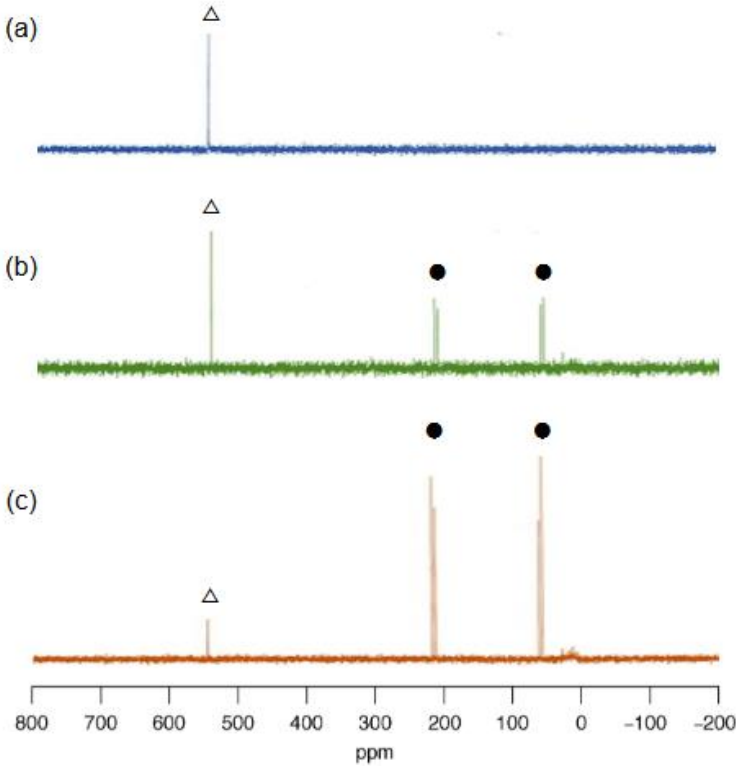

Fig. S1 ^{31}P NMR spectra showing conversion of **1a** (Δ) to **2a** (●) in C_6D_6 at 60 °C under O_2 gas: (a) before reaction, (b) after 8 hours and (c) after 2 days.

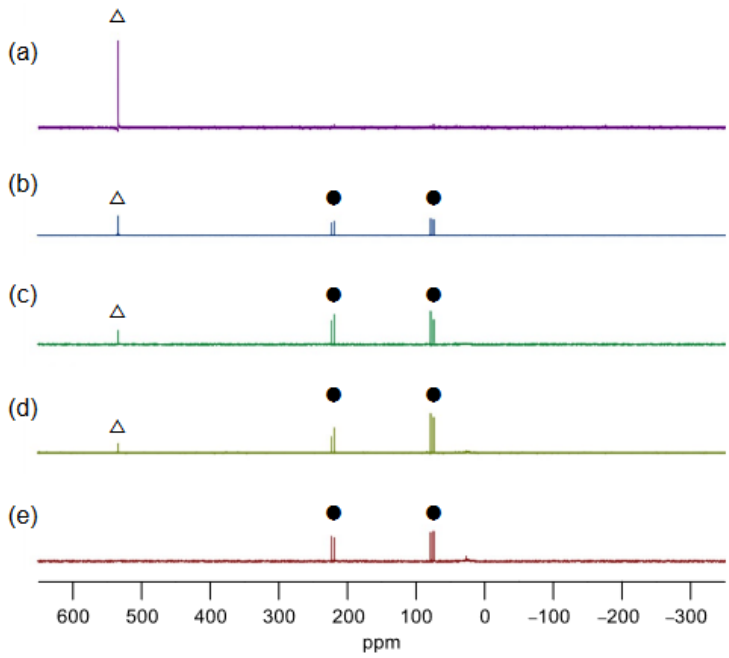

Fig. S2 ^{31}P NMR spectra showing conversion of **1b** (Δ) to **2b** (●) in C_6D_6 at room tempearture under O_2 gas: (a) before reaction, (b) after 4 hours, (c) after 1 day, (d) after 2 days and (e) after 3 days.

2. X-ray Crystallographic Analysis

Crystallographic data of **2a** and **2b** are summarized in Table S1. Single crystals suitable for X-ray diffraction measurements were obtained from toluene for **2a** and from C_6D_6 for **2b** as light yellow blocks.

The single crystals were immersed in oil (Immersion Oil, type B: Code 1248, Cargille Laboratories, Inc.) and mounted on a Rigaku AFC10 diffractometer with a Saturn724 CCD detector for **2a** and a Rigaku XtaLAB P200 with a PILATUS200 K detector for **2b**. The diffraction data were collected using Mo*K*α radiation (λ = 0.71073 Å), which was monochromated by a multi-layered confocal mirror. The specimens were cooled at 100 K in a cold nitrogen stream during the measurements. Bragg spots were integrated and scaled with the programs of CrystalClear[S2] for **2a** and CrysAlisPro[S3] for **2b**. Then, intensities of the equivalent reflections merged for structure analysis.

The structure was solved by a direct method with the programs of SIR2004[S4] for **2a** and SHELXT-2018/2[S5] for **2b**. The structures were refined with a least-squares method on F^2 using SHELXL-2019/2 software.[S6] The anisotropic temperature factors were applied to all non-hydrogen atoms. The hydrogen atoms were put at calculated positions, and refined applying riding models. The detailed crystallographic data have been deposited with the Cambridge Crystallographic Data Centre: Deposition code CCDC 2310280 (**2a**) and 2310282 (**2b**). A copy of the data can be obtained free of charge via www.ccdc.cam.ac.uk/data–request.

The molecular structures of **2a** and **2b** (molecules A and B) are shown in Figs. S3, S5 and S7. The space-filling models of **2a** and **2b** (molecules A and B) are depicted in Figs. S4, S6 and S8.

Table S1 Crystallographic Data for **2a** and **2b**.

	2a	**2b**
formula	$C_{56}H_{90}OP_2$	$C_{48}H_{74}OP_2$
M	841.21	729.01
T / K	100	100
colour	light yellow	light yellow
size, mm	0.136 × 0.118 × 0.067	0.236 × 0.152 × 0.124
crystal system	triclinic	triclinic
space group	P–1 (#2)	P–1 (#2)
a / Å	8.117(2)	10.7135(4)
b / Å	10.258(3)	11.7140(4)
c / Å	15.819(5)	17.7296(6)
α / deg.	89.981(9)	93.270(3)
β / deg.	85.861(8)	90.315(3)
γ / deg.	68.598(7)	102.939(3)
V / Å^3	1222.6(6)	2164.62(13)
Z	1	2
D_x / g cm^{-3}	1.143	1.118
reflections collected	23732	102563
unique reflections	7304	11259
refined parameters	293	504
GOF on F^2	1.083	1.051
$R1$ [$I > 2\sigma(I)$][a]	0.0662	0.0662
w$R2$ (all data)[b]	0.1508	0.1532
$\Delta\rho_{min,\ max}$ / e Å^{-3}	−0.309, 0.439	− 0.421, 0.350

[a] $R1 = \Sigma\ ||Fo| - |Fc|| / \Sigma\ |Fo|$, [b] $wR2 = [\Sigma\ \{w(Fo^2–Fc^2)^2 / \Sigma\ w(Fo^2)^2\}]^{1/2}$

(a)

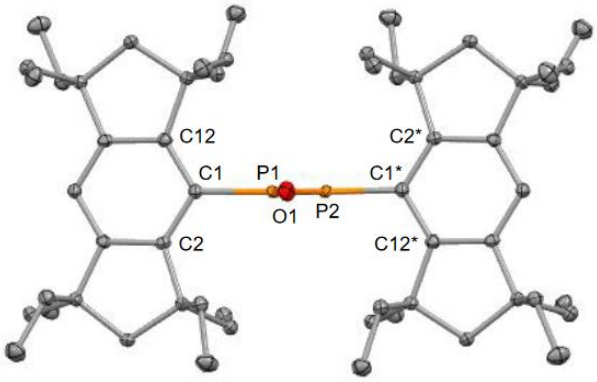

(b)

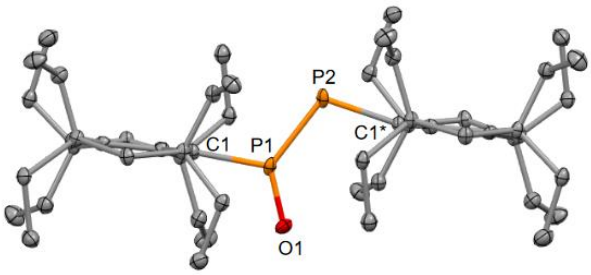

Fig. S3 Molecular structures of **2a**; (a) side view, (b) top view. The thermal ellipsoids are shown in the 50% probability level. All hydrogen atoms and disordered O and P atoms are omitted for clarity. Selected atomic distances (Å), bond angles (deg) and torsion angles (deg): P1–P2 = 2.040(2), P1–O1 = 1.455(8), P1–C1 = 1.851(13), P2–C1* = 1.892(13), O1–P1–C1 = 113.5(6), O1–P1–P2 = 129.7(5), C1–P1–P2 = 116.8(3), C1*–P2–P1 = 108.8(3), P2–P1–C1–C2 = –102.1(2), P2–P1–C1–C12 = 85.3(3), O1–P1–C1–C2 = 78.7(7), O1–P1–C1–C12 = –94.0(7), P1–P2–C1*–C2* = 106.2(5), P1–P2–C1*–C12* = –90.8(5), C1–P1–P2–C1* = –178.5(5) and O1–P1–P2–C1* = 0.5(11).

(a)

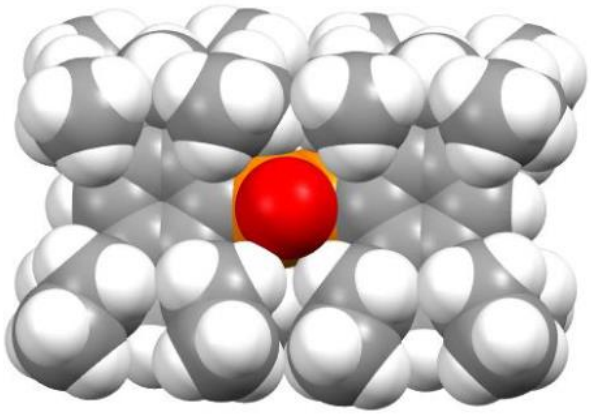

(b)

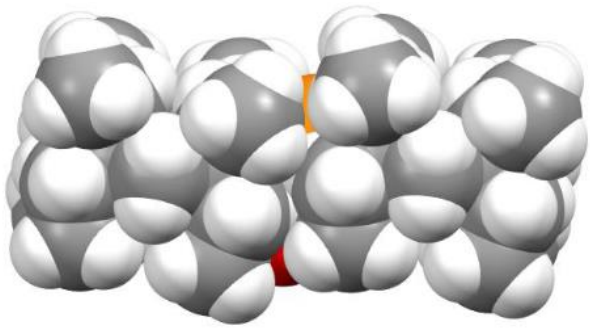

Fig. S4 Space filling models of **2a**; (a) side view, (b) top view: orange, phosphorus; red, oxygen; gray, carbon; white, hydrogen.

(a)

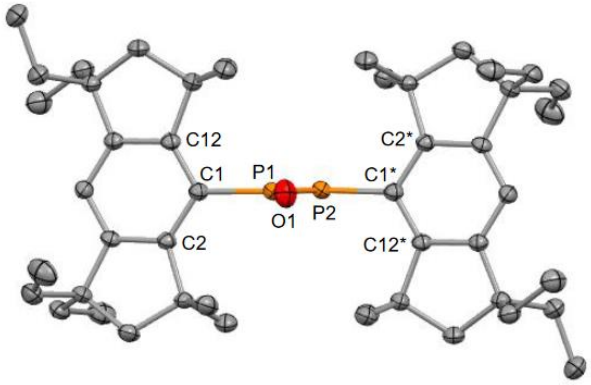

(b)

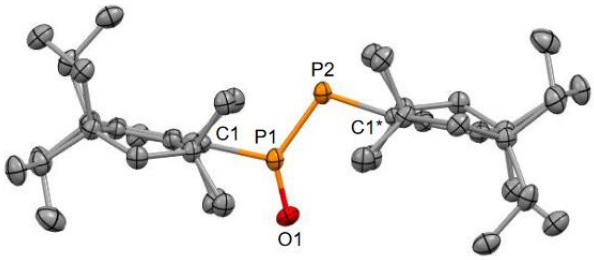

Fig. S5 Molecular structures of **2b** (molecule A); (a) side view, (b) top view. The thermal ellipsoids are shown in the 50% probability level. All hydrogen atoms and disordered O and P atoms are omitted for clarity. Selected atomic distances (Å), bond angles (deg) and torsion angles (deg): P1–P2 = 2.0377(14), P1–O1 = 1.446(12), P1–C1 = 1.842(16), P2–C1* = 1.864(15), O1–P1–C1 = 114.9(9), O1–P1–P2 = 131.7(6), C1–P1–P2 = 113.3(4), C1*–P2–P1 = 106.9(4), P2–P1–C1–C2 = 99.0(3), P2–P1–C1–C12 = –86.1(4), O1–P1–C1–C2 = –79.6(11), O1–P1–C1–C12 = 95.4(10), P1–P2–C1*–C2* = 103.1(3), P1–P2–C1*–C12* = –89.3(3), C1–P1–P2–C1* = 178.3(7) and O1–P1–P2–C1* = 0(2).

(a)

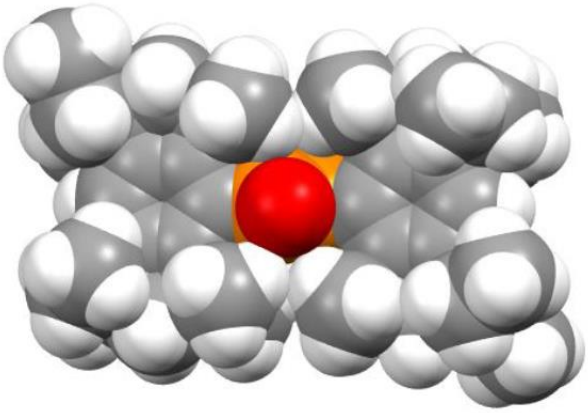

(b)

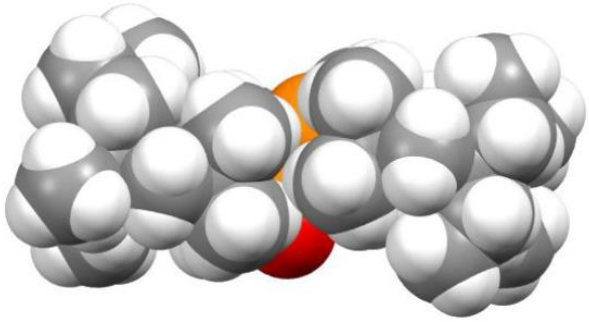

Fig. S6 Space filling models of **2b** (molecule A); (a) side view, (b) top view: orange, phosphorus; red, oxygen; gray, carbon; white, hydrogen.

(a)

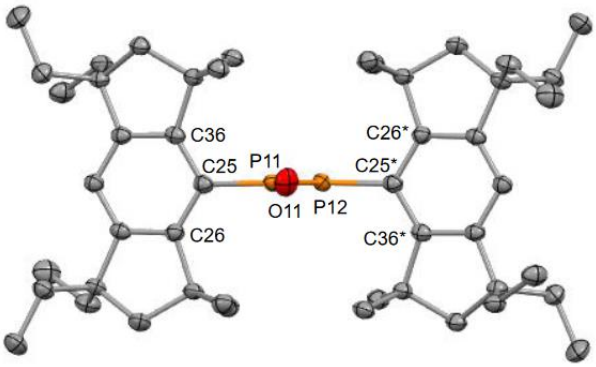

(b)

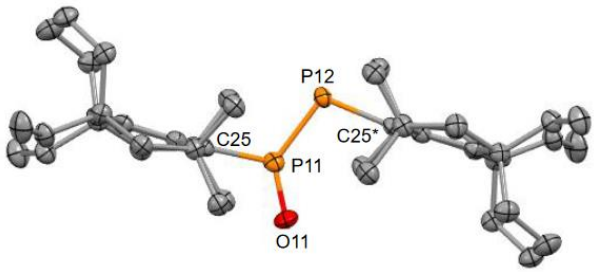

Fig. S7 Molecular structures of **2b** (molecule B); (a) side view, (b) top view. The thermal ellipsoids are shown in the 50% probability level. All hydrogen atoms and disordered O and P atoms are omitted for clarity. Selected atomic distances (Å), bond angles (deg) and torsion angles (deg): P11–P12 = 2.036(3), P11–O11 = 1.471(5), P11–C25 = 1.789(9), P12–C25* = 1.917(8), O11–P11–C25 = 114.2(5), O11–P11–P12 = 130.7(4), C25–P11–P12 = 115.1(2), C25*–P12–P11 = 104.6(2), P12–P11–C25–C26 = –88.2(3), P12–P11–C25–C36 = 90.5(3), O11–P11–C25–C26 = 91.9(6), O11–P11–C25–C36 = –89.3(5), P11–P12–C25–C26 = 95.3(4), P11–P12–C25–C36 = –96.0(4), C25–P11–P12–C25* = 177.9(4) and O11–P11–P12–C25* = –2.3(8).

(a)

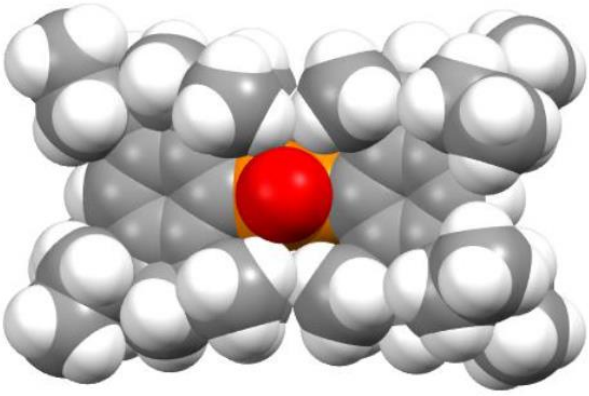

(b)

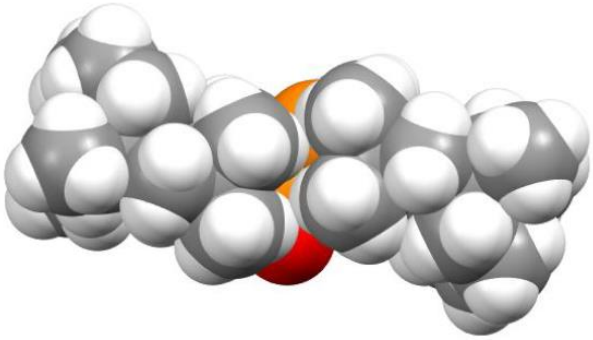

Fig. S8 Space filling models of **2b** (molecule B); (a) side view, (b) top view: orange, phosphorus; red, oxygen; gray, carbon; white, hydrogen.

3. Theoretical Calculations

The geometry optimization of **1a**, **1b**, **2a**, **2b**, (Eind)(O_2)P=P(Eind) (**3a**) and (EMind)(O_2)P=P(EMind) (**3b**) were performed at the B3LYP-D3/6-31G(d,p) level of theory using Gaussian 09 program package.[S7] The optimized structures and selected structural parameters of **1a**, **1b**, **2a**, **2b**, **3a** and **3b** are shown in Figs. S9–S14. Selected molecular orbitals (MOs) and their energy levels of **1a**, **1b**, **2a** and **2b** are shown in Figs. S15–S18. The Wiberg bond index (WBI)[S8] and natural bond orbital (NBO)[S9] charge distribution of **1a**, **1b**, **2a**, **2b**, **3a** and **3b** are shown in Figs. S19–S24. The ^{31}P chemical shifts were calculated for the optimized geometry of **2a** and **2b** using the gauge-independent atomic orbital (GIAO) method (δ = 0.0 ppm for H_3PO_4) (Figs. S25 and S26).

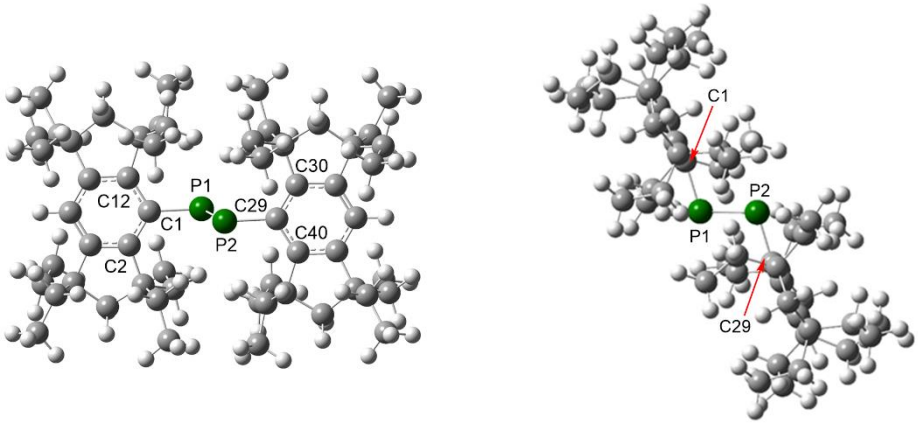

Fig. S9 Optimized structures of **1a** (C_1 symmetry): side view (left) and top view (right). Selected atomic distances (Å), bond angles and torsion angles (deg): P1–P2 = 2.0651, P1–C1 =1.8985, P2–C29 = 1.8985, P2–P1–C1 = 107.28, P1–P2–C29 = 107.29, P2–P1–C1–C2 = 87.51, P2–P1–C1–C12 = –105.22, P1–P2–C29–C30 = 105.21, P1–P2–C29–C40 = –87.51 and C1–P1–P2–C29 = 180.00.

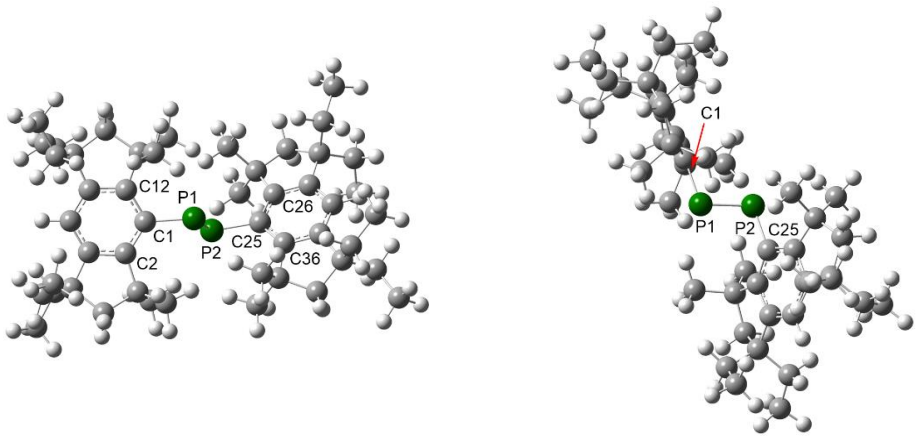

Fig. S10 Optimized structures of **1b** (C_1 symmetry): side view (left) and top view (right). Selected atomic distances (Å), bond angles and torsion angles (deg): P1–P2 = 2.0521, P1–C1 =1.8701, P2–C25 = 1.8710, P2–P1–C1 = 105.26, P1–P2–C25 = 103.13, P2–P1–C1–C2 = 71.18, P2–P1–C1–C12 = –116.59, P1–P2–C25–C26 = 69.35, P1–P2–C25–C36 = –114.55 and C1–P1–P2–C25 = 174.37.

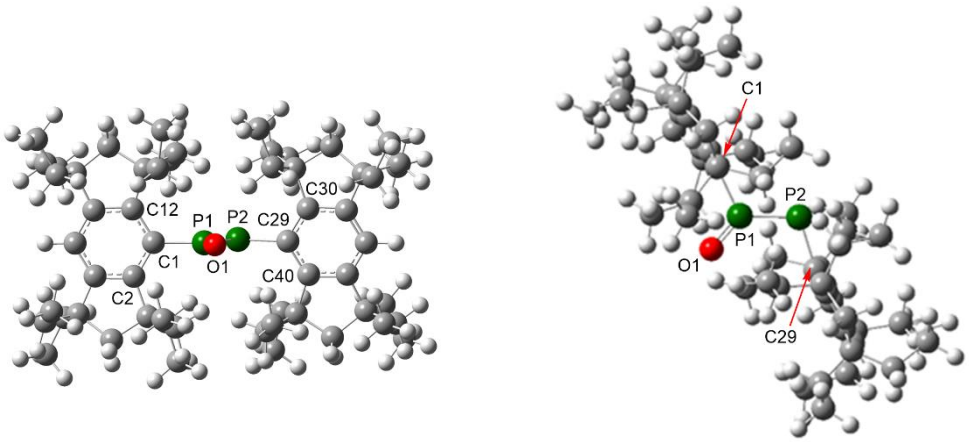

Fig. S11 Optimized structure of **2a** (C_1 symmetry): side view (left) and top view (right). Selected atomic distances (Å), bond angles and torsion angles (deg): P1–P2 = 2.0569, P1–O1 = 1.5046, P1–C1 = 1.8596, P2–C29 = 1.8937, P2–P1–C1 = 116.55, P2–P1–O1 = 129.32, C1–P1–O1 = 114.11, P1–P2–C29 = 108.70, P2–P1–C1–C2 = 91.17, P2–P1–C1–C12 = –97.24, O1–P1–C1–C2 = –90.13, O1–P1–C1–C12 = 81.47, P1–P2–C29–C30 = 104.73, P1–P2–C29–C40 = –88.20, C1–P1–P2–C29 = –178.94, O1–P1–P2–C29 = 2.59.

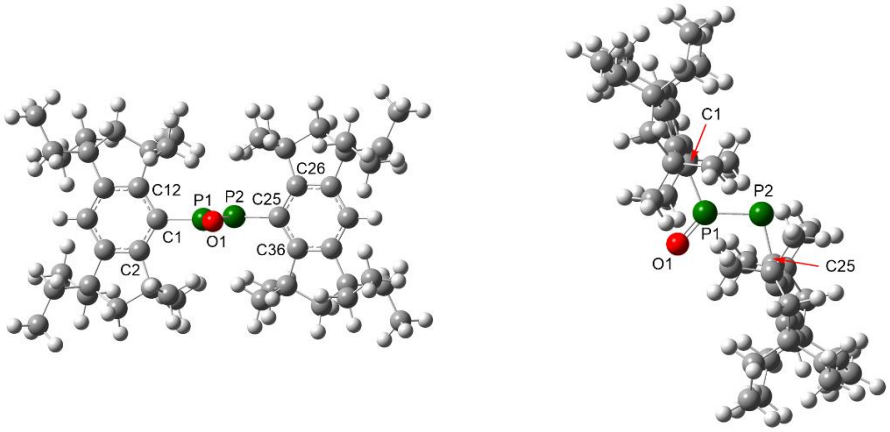

Fig. S12 Optimized structure of **2b** (C_1 symmetry): side view (left) and top view (right). Selected atomic distances (Å), bond angles and torsion angles (deg): P1–P2 = 2.0464, P1–O1 = 1.5021, P1–C1 = 1.8450, P2–C25 = 1.8808, P2–P1–C1 = 112.66, P2–P1–O1 = 130.06, C1–P1–O1 = 117.28, P1–P2–C25 = 104.20, P2–P1–C1–C2 = 90.75, P2–P1–C1–C12 = –90.73, O1–P1–C1–C2 = –89.26, O1–P1–C1–C12 = 89.26, P1–P2–C25–C26 = 93.58, P1–P2–C25–C36 = –93.46, C1–P1–P2–C25 = –179.99 and O1–P1–P2–C25 = 0.03.

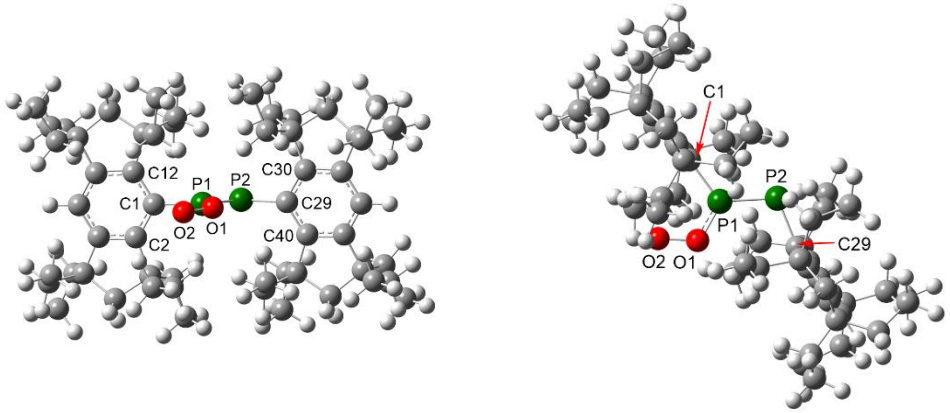

Fig. S13 Optimized structure of **3a** (C_1 symmetry): side view (left) and top view (right). Selected atomic distances (Å), bond angles and torsion angles (deg): P1–P2 = 2.0694, P1–O1 = 1.6038, O1–O2 = 1.4170, P1–C1 = 1.8378, P2–C29 = 1.8852, P2–P1–C1 = 123.25, P2–P1–O1 = 122.66, C1–P1–O1 = 114.08, P1–P2–C29 = 108.85, O2–O1–P1 = 116.91, P2–P1–C1–C2 = 86.32, P2–P1–C1–C12 = –96.52, O1–P1–C1–C2 = –92.62, O1–P1–C1–C12 = 84.54, P1–P2–C29–C30 = 103.08, P1–P2–C29–C40 = –90.67, C1–P1–P2–C29 = –178.04, O1–P1–P2–C29 = 0.81, O2–O1–P1–P2 = –176.94, O2–O1–P1–C1 = 2.01.

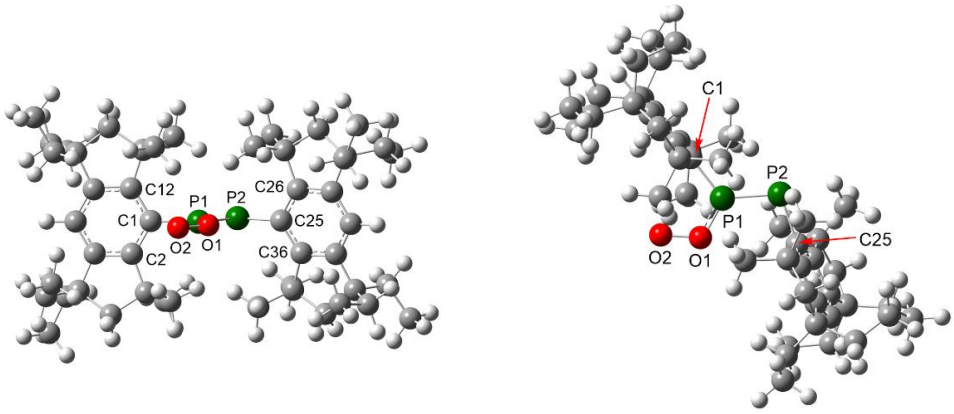

Fig. S14 Optimized structure of **3b** (C_1 symmetry): side view (left) and top view (right). Selected atomic distances (Å), bond angles and torsion angles (deg): P1–P2 = 2.0627, P1–O1 = 1.6031, O1–O2 = 1.4191, P1–C1 = 1.8254, P2–C25 = 1.8805, P2–P1–C1 = 123.74, P2–P1–O1 = 123.32, C1–P1–O1 = 112.94, P1–P2–C25 = 104.66, O2–O1–P1 = 115.57, P2–P1–C1–C2 = 93.70, P2–P1–C1–C12 = –91.70, O1–P1–C1–C2 = –86.99, O1–P1–C1–C12 = 87.61, P1–P2–C25–C26 = 103.16, P1–P2–C25–C36 = –86.08, C1–P1–P2–C25 = –179.75, O1–P1–P2–C25 = 1.01, O2–O1–P1–P2 = –179.47, O2–O1–P1–C1 = 1.22.

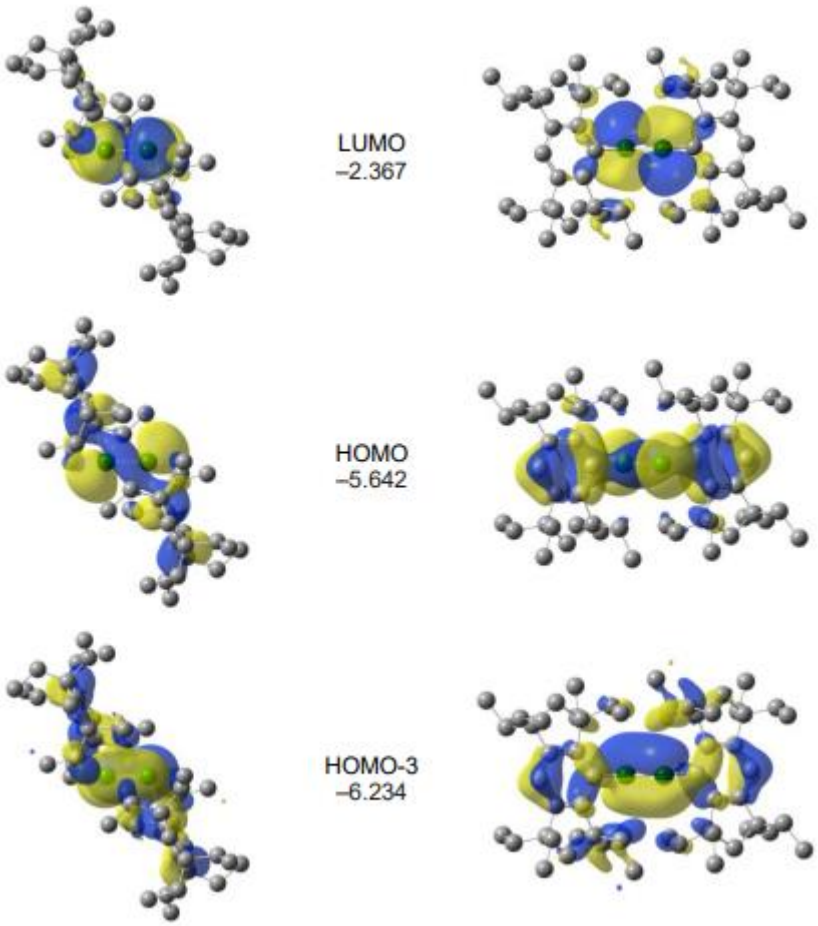

Fig. S15 Selected molecular orbitals and their energy levels (eV) of **1a**; top views (left), front views (right).

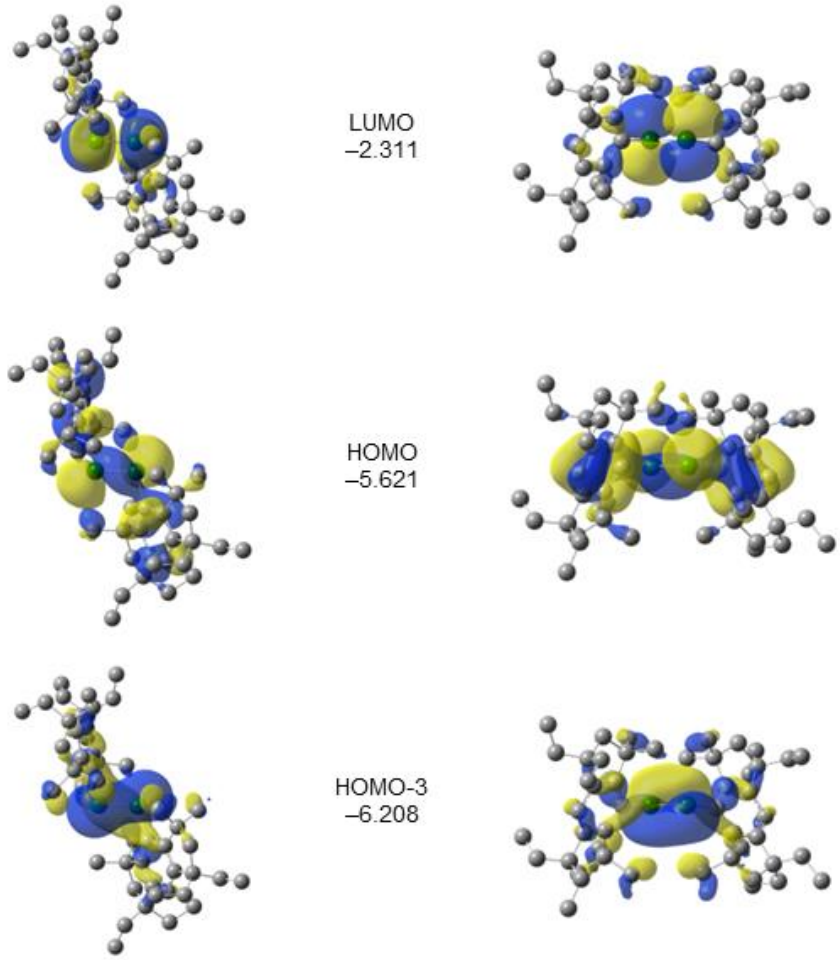

Fig. S16 Selected molecular orbitals and their energy levels (eV) of **1b**; top views (left), front views (right).

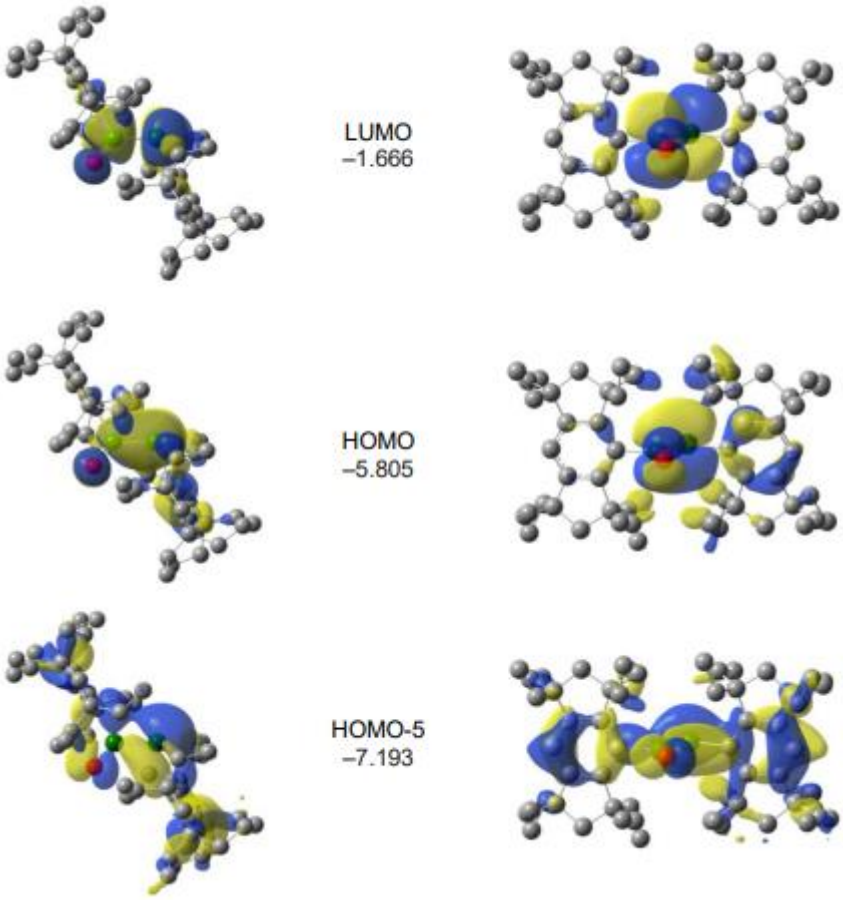

Fig. S17 Selected molecular orbitals and their energy levels (eV) of **2a**; top views (left), front views (right).

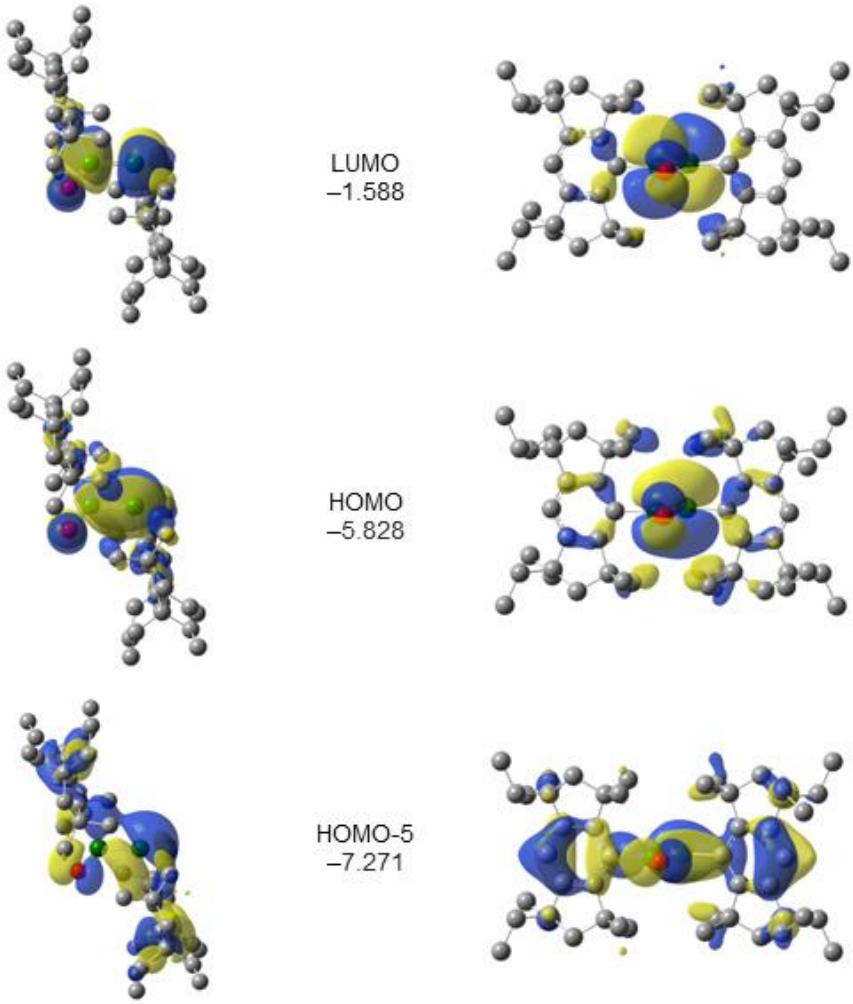

Fig. S18 Selected molecular orbitals and their energy levels (eV) of **2b**; top views (left), front views (right).

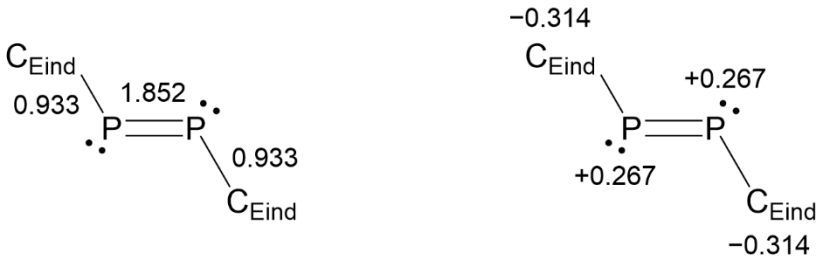

Fig. S19 WBI (left) and NBO charge distribution (right) of **1a**.

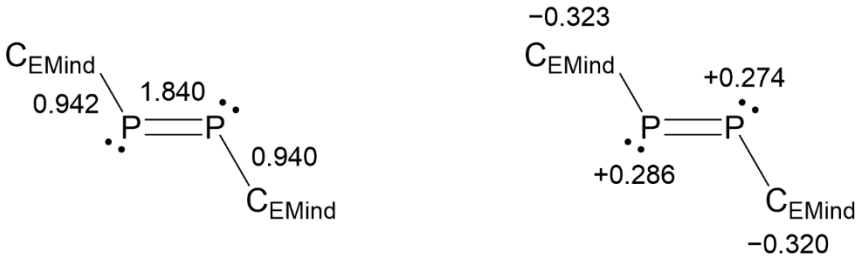

Fig. S20 WBI (left) and NBO charge distribution (right) of **1b**.

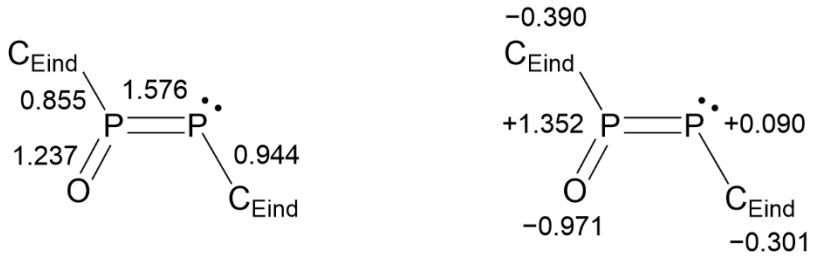

Fig. S21 WBI (left) and NBO charge distribution (right) of **2a**.

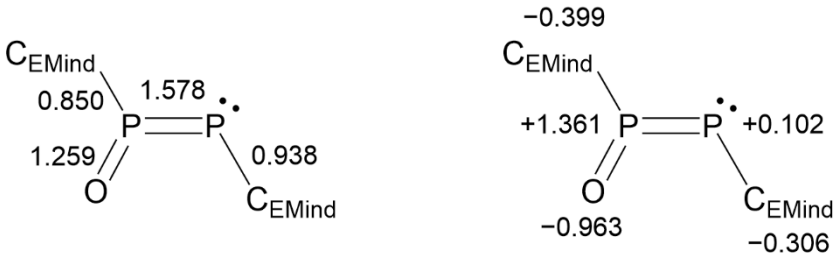

Fig. S22 WBI (left) and NBO charge distribution (right) of **2b**.

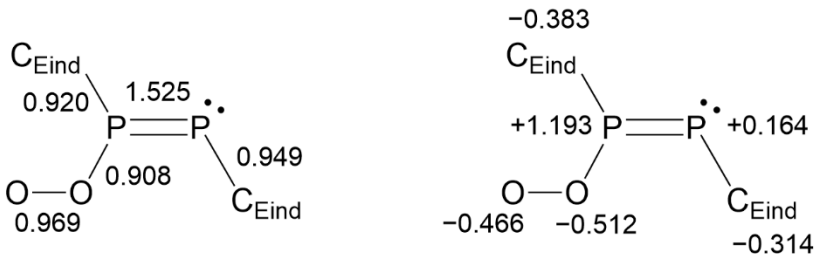

Fig. S23 WBI (left) and NBO charge distribution (right) of **3a**.

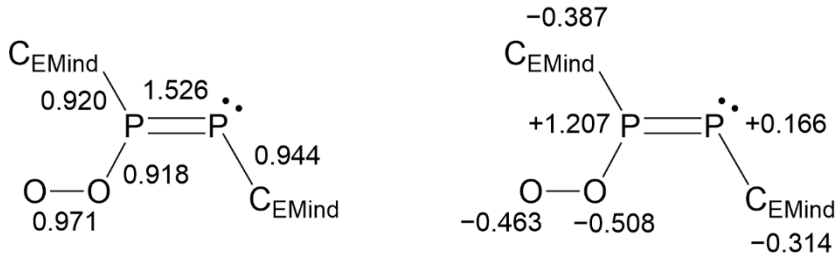

Fig. S24 WBI (left) and NBO charge distribution (right) of **3b**.

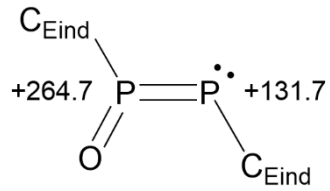

Fig. S25 The calculated ^{31}P chemical shifts (ppm) of **2a** (B3LYP-D3/6-31G(d,p) level).

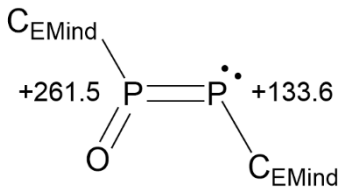

Fig. S26 The calculated ^{31}P chemical shifts (ppm) of **2b** (B3LYP-D3/6-31G(d,p) level).

5. References

S1 B. Li, S. Tsujimoto, Y. Li, H. Tshuji, K. Tamao, D. Hashizume and T. Matsuo, *Heteroat. Chem*., 2014, **25**, 612.

S2 Crystalclear: Rigaku/MSC. Inc., 9009 New Trails Drive, The Woodlands TX 77381, USA (2005).

S3 CrysAlisPro: Agilent Technologies Ltd, Yarnton, Oxfordshire, England, 2014.

S4 SIR2004: M. C. Burla, M. Camalli, B. Carrozzini, G. L. Cascarano, C. Giacovazzo, A. Guagliardi, A. G. G. Moliterni, G. G. Polidori and R. Spagna, *J. Appl. Cryst*., 2003, **36**, 1103.

S5 SHELXT-2018/2: G. M. Sheldrick, *Acta Crystallogr., Sect. A: Found. Adv*., 2015, **71**, 3.

S6 SHELXL-2019/2: G. M. Sheldrick, *Acta Crystallogr., Sect. C: Struct. Chem*., 2015, **71**, 3.

S7 Gaussian 09, Revision B.01: M. J. Frisch, G. W. Trucks, H. B. Schlegel, G. E. Scuseria, M. A. Robb, J. R. Cheeseman, G. Scalmani, V. Barone, B. Mennucci, G. A. Petersson, H. Nakatsuji, M. Caricato, X. Li, H. P. Hratchian, A. F. Izmaylov, J. Bloino, G. Zheng, J. L. Sonnenberg, M. Hada, M. Ehara, K. Toyota, R. Fukuda, J. Hasegawa, M. Ishida, T. Nakajima, Y. Honda, O. Kitao, H. Nakai, T. Vreven, J. A. Jr. Montgomery, J. E. Peralta, F. Ogliaro, M. Bearpark, J. J. Heyd, E. Brothers, K. N. Kudin, V. N. Staroverov, T. Keith, R. Kobayashi, J. Normand, K. Raghavachari, A. Rendell, J. C. Burant, S. S. Iyengar, J. Tomasi, M. Cossi, N. Rega, J. M. Millam, M. Klene, J. E. Knox, J. B. Cross, V. Bakken, C. Adamo, J. Jaramillo, R. Gomperts, R. E. Stratmann, O. Yazyev, A. J. Austin, R. Cammi, C. Pomelli, J. W. Ochterski, R. L. Martin, K. Morokuma, V. G. Zakrzewski, G. A. Voth, P. Salvador, J. J. Dannenberg, S. Dapprich, A. D. Daniels, O. Farkas, J. B. Foresman, J. V. Ortiz, J. Cioslowski and D. J. Fox, Gaussian, Inc., Wallingford CT, 2010.

S8 O. V. Sizova, L. V. Skripnikov and A. Yu. Sokolov, *THEOCHEM*, 2008, **870**, 1.

S9 E. D. Glendening, J. K. Badenhoop, A. E. Reed, J. E. Carpenter, J. A. Bohmann, C. M. Morales, P. Karafiloglou, C. R. Landis and F. Weinhold, NBO 7.0;

Theoretical Chemistry Institute; University of Wisconsin: Madison, 2018.